Observation of positive and negative oxygen ions during electron bombardment of oxygen-covered Mo (100) surfaces

Ming L. Yu*
Brookhaven National Laboratory, Upton, New York 11973
(Received 30 January 1979)

Electron-stimulated desorption of both positive and negative ions from oxygen-covered Mo (100) surfaces was investigated. Two adsorption states, α and β, were identified. For the high-ion-yield α state, the O^- to O^+ yield ratio varied with both temperature and oxygen coverage, indicating changes in the nature of this state. For the low-ion-yield β state, the O^+-ion yield showed reversible thermal enhancement, possibly caused by the migration of oxygen atoms in and out of the Mo surface. A velocity-dependent isotope effect was also observed for both positive and negative oxygen ions. The phenomenon is discussed in the framework of Franck-Condon transitions.

I. INTRODUCTION

Although electron-stimulated desorption (ESD) is now a very well-known phenomenon, most of the reported experiments have dealt exclusively with desorbed positive and neutral particles.[1] Electron desorption of negative ions was first reported by Moore.[2] Recently more conclusive evidence was reported by Ayukhanov and Turmashev,[3] and also by Hock and Lichtman.[4] In this paper we report a detailed comparison between the positive- and negative-oxygen-ion yields during electron desorption of oxygen overlayers on Mo (100) surfaces. This is probably the first systematic investigation of electron desorption of negative ions from a chemisorption system. Various properties including the oxygen-coverage dependences, ion-energy distributions (IED) of the ion yields, were measured. It was observed that the O^- to O^+ yield ratio depended on the original adsorbate state of the desorbed atoms. The isotope effect of both O^+ and O^- desorption was found to have an interesting ion-energy dependence. The implication on the mechanism of negative ion desorption is discussed.

Numerous ESD studies of oxygen on Mo had been reported.[5-7] The O-Mo(100) system was also studied extensively with LEED and other surface analytical techniques.[8-9] Unfortunately, very little ESD investigation on this system was performed.[10] Therefore, we also report the results which have significance on the O-Mo(100) chemisty. The LEED structures of the oxygen overlayers at various temperatures were carefully monitored during the ESD experiment so that comparison with other reported experiments could be made.

II. EXPERIMENTAL

The experiment was performed inside an ion-pumped ultrahigh vacuum (UHV) system with a base pressure in the upper 10^{-11}-Torr range. A residual gas analyzer was used to monitor partial pressures. A LEED electron gun provided the low-energy electron beams. The desorbed ions were mass analyzed by a quadrupole mass spectrometer. The detector was a channeltron operated in the counting mode. The sample was a high-purity Mo(100) single crystal in the form of 0.025-in.-thick, 0.38-in.-diam disc. Two 0.625-mm Mo wires were spot welded to the back of the sample. The wires were in turn clamped to two Mo support rods. The crystal was resistively heated and the sample temperature was monitored with a W-26-at.%-Re–W-5-at.5%-Re thermocouple which was also spot welded to the back of the sample. The sample cleaning procedure involved heating the sample to 900 °C in the 10^{-6} Torr of O_2 for an hour to remove carbon, followed by flash heating to 1700 °C to remove the oxygen. The above procedure was repeated when necessary. The chamber was also equipped with LEED and Auger-electron spectrometer (AES) for sample surface characterization.

The angle of incidence of the electron beam was 71°. The typical electron current was 500 nA. The electron current density was estimated to be less than 10 $\mu A/cm^2$. The ions were detected with the sample surface normal to the mass spectometer axis. The ionizer of the mass spectometer was replaced by an energy analyzer[11] operated in the constant energy width mode. The full width at half maximum (FWHM) of the pass band was about 1.3 eV. The mass spectrometer axis was always maintained at a constant potential with respect to the pass energy to ensure constant transmission for ions of different energies. The sample was at ground potential and no extraction voltage was used. The sample was actually carefully shielded from the electric fields of the ion optics so that the angular distribution of the ions was not affected during the energy scan. To obtain

the total yield within the cone of acceptance, the pass energy of the energy analyzer was scanned linearly from 0 to 12 eV during the counting period (10 sec) so that at least 95% of the ion-energy distribution (IED) was covered. This energy-integrated yield was used an an indicator for the relative magnitudes of the ion desorption cross sections. The mass spectrometer was programmed so that it was able to look at any two different ionic species in alternation. In this way, it was possible to measure both O^- and O^+ yields simultaneously as a function of adsorbate dosage during each run. Data at elevated temperatures were taken with a pulsed heating technique. The mass spectrometer was gated off during the heating pulse to avoid spurious magnetic field effects from the heating current. Pulsed heating was also used to observe LEED patterns at elevated temperatures. In this case, a high voltage synchronized with the heating current was applied to the first grid of the LEED optics to repel the diffracted electrons during the heating cycle.

III. RESULTS

A. Room temperature

The oxygen overlayer showed all the now well-documented LEED structures. At room temperature, the oxygen overlayer first forms a diffuse $c(2\times 2)$ pattern at about 0.5 L (1 langmuir = 10^{-6} Torr sec) O_2 exposure. Then streaks at half order spots appeared, to be followed by integral streaks at exposures above 1L. At 2-L exposure, only the integral streaks remained. The ESD O^+ yield rose slowly with oxygen coverage. These different stages of chemisorption were not reflected in the O^+ yield. The O^- yield was still too small to be detected. After 3.5-L exposure, the O^+ and O^- yields both rose very rapidly (Fig. 1). We shall designate the initial low-ion-yield state of chemisorption as the β state and the high-ion-yield state as the α state.[6] This ESD behavior is very similar to that reported for the O-W(100) system.[12] The only difference is that no β-state yield maximum or minimum was observed for the O-Mo(100) system. Above 2-L exposure the integral streaks of the LEED pattern increased in intensity. After 3.5-L exposure, the streaks began to weaken and gradually transformed into a $p(1\times 1)$ structure at saturation. Both O^- and O^+ yields increased rapidly after the onset of the α state. Again the α state ion yields did not show any indication of the different chemisorption stages. Both O^- and O^+ yields saturated at about 6 L. The O^- yield was generally about two orders of magnitude lower than the O^+ yield. The energy distributions of the oxygen ions from an oxygen saturated Mo(100) surface were also measured. The O^+ yield peaked at about 6 eV while the O^- yield peaked at about 7.5 eV. The shape of the IED's did not change noticeably with oxygen coverage.

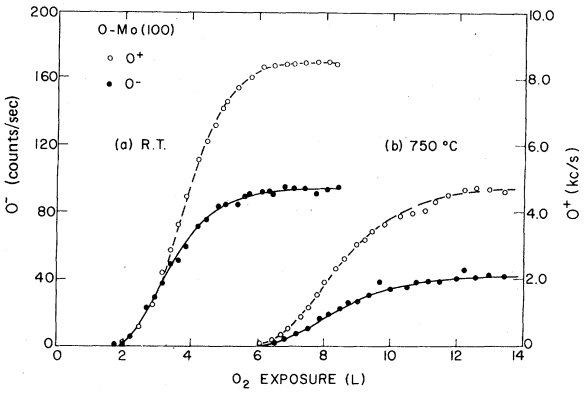

FIG. 1. O^- and O^+ yields as a function of O_2 exposure at (a) room temperature and (b) 750 °C. The onset of the high-ion-yield α state was strongly temperature dependent.

B. Higher temperatures

The onset of the α state moved to increasingly higher oxygen exposures when the temperature of the sample was raised (Fig. 1). The oxygen-coverage dependence also suggested that the onset

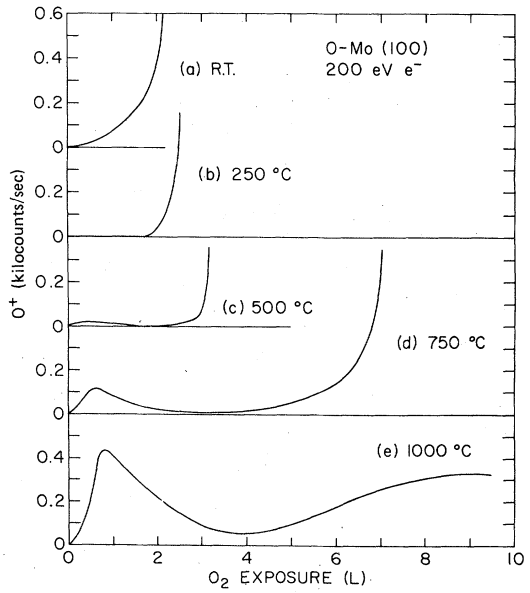

FIG. 2. β-state O^+ yield as a function of O_2 exposure at various temperatures. Note that the yield was first suppressed at 250 °C and then enhanced significantly at higher temperatures. The β-state O^+ yield maximum also occurred at roughly the same oxygen exposure at all temperatures.

was the same for both O^- and O^+ ion yields at all temperatures. The β-state O^+ yield disappeared rapidly when heated above the room temperature. Figure 2 shows the β-state O^+ yields at various temperatures. At 250 °C the β-state O^+ signal was below the detector sensitivity. The oxygen overlayer formed a $c(4\times4)$ structure at about 0.75-L exposure. At about 1 L, the $c(4\times4)$ structure started to disappear. With further increase in exposure, there was a strong, diffuse, ring shaped background affecting especially the (01) and the other three equivalent spots. This diffuse background gradually disappeared at higher coverages. At 3 L only a $p(1\times1)$ structure with reduced spot intensity remained. The onset of the α state for ESD was at about 2-L exposure. The saturation O^- and O^+ yields were a few percent higher than the room-temperature values. The O^- to O^+ ratio was also higher at 250 °C.

There were many interesting LEED structures at 500 °C. When the exposure was below 1 L a $c(4\times4)$ pattern was observed. But soon, the $c(4\times4)$ was gradually replaced by the strong diffuse ring background as was observed at 250 °C. At about 2-L exposure, out of the ring background a sharp $(\sqrt{5}\times\sqrt{5})R\ 26°34'$ structure emerged. The spot intensity was maximum at about 2.5-L exposure. Apparently the diffuse ring background was a precursor to this $\sqrt{5}\times\sqrt{5}$ structure. Beyond 2.5-L exposure, the $\sqrt{5}\times\sqrt{5}$ pattern gradually got dimmer and there were streaks an integral spots. At 3.5 L, the $p(2\times2)$ structure started to appear. This structure lasted beyond 6-L exposure. Further oxygen exposure weakened the $p(2\times2)$ structure and a $p(1\times1)$ pattern with diffuse background resulted at 8 L. The onset of the ESD α state was at about 3 L, that is, just before the formation of the $p(2\times2)$ structure.

The interesting observation, however, was the reappearance of a β-state O^+ yield which was suppressed at 250 °C. This O^+ yield reached a maximum at about 0.75 L and then went back to zero again before the onset of the α state. This was somewhat similar to the β-state yield maximum observed for O-W(100).[12,13] The distinct difference was that the β-state yield maximum for O-Mo(100) was strongly temperature dependent as shown in Fig. 2. At 1000 °C, the β-state O^+ maximum was comparable to the α-state O^+ yield. The temperature dependence suggested a thermal excitation mechanism. Figure 3 shows an Arrhenius plot of the β-state O^+ yield maximum. The linear behavior suggested a well-defined excitation energy of about 0.6 eV. The β-state O^+ peak occurred roughly at 0.75 L at all temperatures. This suggested that the yield maximum correlated with the $c(2\times2)$ structure at room temperature and the $c(4\times4)$ structure at higher temperatures.

After 1-L exposure at 750 °C, we observed the $c(4\times4)$ structure only when we allowed the sample to cool down to about 500 °C. But at 2-L exposure, the $\sqrt{5}\times\sqrt{5}$ structure appeared clearly even at 750 °C. Further exposure to oxygen caused the $\sqrt{5}\times\sqrt{5}$ to disappear, reverting back to the $p(1\times1)$ at 2.5 L, before forming the $p(2\times2)$ structure which lasted up to 5-L exposure. Then it went back to $p(1\times1)$ with a diffuse background. The onset of the α state O^+ yield was at about 6 L, which was after the disappearance of the $p(2\times2)$ structure.

IV. DISCUSSIONS

The correlation with the LEED structures that the ESD oxygen ion yields from submonolayers of oxygen on Mo(100) was very small. This is consistent with the suggestion[6] that strongly chemisorbed oxygen atoms have small ionic desorption cross sections. The β state probably consists of the first monolayer of oxygen atoms. We also suspect that the initial β-state yield observed at room temperature was a contribution from a few loosely bound α-state oxygen atoms that happened to be present in small quantities ($\simeq 1\%$) even at low oxygen coverages. This can explain why this β-state O^+ yield disappeared with only slight increase in temperature. The thermally enhanced β-state O^+ yields observed at higher temperatures were probably true contributions from the strongly chemisorbed layer.

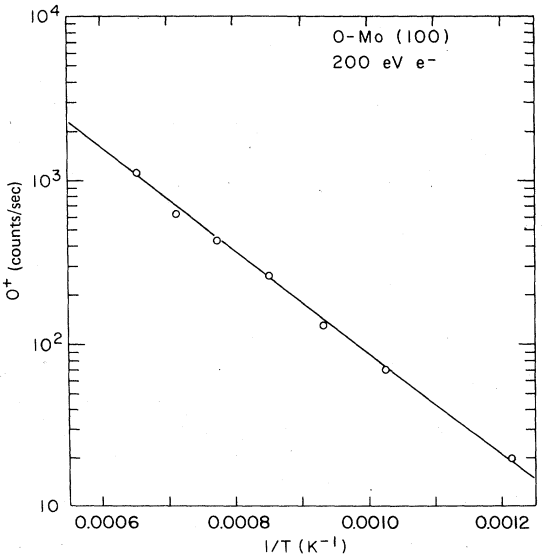

FIG. 3. Log plot of the β-state O^+yield maximum vs $1/T$. The linear relation implies a thermal activation process with an activation energy about 0.6 eV.

Room-temperature work function measurements showed that the room-temperature $c(2\times2)$ structure was characterized by a decrease in work function.[9] A proposed explanation was that at low oxygen coverages, the oxygen atoms penetrated into the surface layer of Mo atoms. If this was the case, it is not hard to understand why the β-state O^+ yield at low temperatures (e.g., 250 °C) was practically zero. The oxygen ion, even if desorbed, would have an extremely high probability of being neutralized during its exit from the metal lattice. A possible explanation of the thermal enhancement of the β-state O^+ yield is that the oxygen atoms were thermally excited to migrate onto the Mo surface where the neutralization probability was lower. The excitation energy was 0.6 eV (Fig. 3). This would imply a rise in the work function at high temperatures. Unfortunately it was not possible in this experiment to measure the work function at high temperatures. However, it was observed that between 700 and 1300 °C the β-state O^+ IED peak energy shifted down by about 1 eV, consistent with a rising sample work function. This is probably the first measurement of the excitation energy required for this type of migration using ESD. There is also the suspicion that the gradual transformation from the $c(2\times2)$ to the $c(4\times4)$ LEED structure with temperature was associated with this thermal enhancement. Aside from the correlation of the yield maximum with the $c(4\times4)$ structure, there was no other apparent indication of a strong dependence of O^+ yield with surface structure in the β state. The ion yields failed to reflect subtle changes in the chemisorption process.

The onset of the α state moved to increasingly higher oxygen exposures as the temperature of the sample was raised. However, the α state did not show any strong association with any particular LEED structure. The α-state yields decreased rapidly with rise in temperature at high temperatures, showing again that the oxygen atoms contributing to the α state yields were weakly bound. As shown in Fig. 2, at 1000 °C, the β-state O^+ yield was actually thermally enhanced, showing the distinct difference between the α and β states. The onset of both β-state O^- and O^+ yields were practically simultaneous. The coverage dependences were also very similar. We suspect that both O^- and O^+ ions originated from the adsorbed oxygen atoms at similar sites. We also found that the O^- to O^+ yield ratio was a function of both temperature and coverage. Figure 4 shows plots of the O^- yields versus the corresponding O^+ yields at various temperatures. At room temperature, the O^- to O^+ ratio was not constant. The ratio decreased at high coverages, indicating a gradual change in the character of the α state. At 250 °C, the O^- to O^+ ratio initially was the same as the room-temperature value at low coverages, but exceeded the room-temperature values at higher coverages. The saturation ion yields were also higher at this temperature. At 500 °C, the O^- to O^+ ratio went back to the room-temperature values. At 750 °C, the O^- to O^+ ratio was constant and was less than those at lower temperatures. The constant ratio seemed to imply that the α state was no longer changing with coverage. So with both the positive and negative ion yields, we can conveniently monitor qualitative chemisorption changes which would be difficult with the positive ion yields only. With further theoretical understanding in the future, quantitative interpretation should be possible.

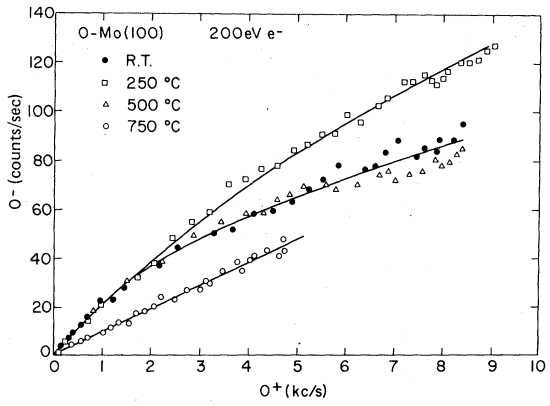

FIG. 4. O^- vs O^+ plots for the α state at varous temperatures. The curves show that the O^- to O^+ yield ratio was a function of both coverage and temperature.

V. ISOTOPE EFFECT

With the observation of the negative ions, we used this opportunity to look at the ion desorption and neutralization process more carefully. There are two current theories for the electron desorption of positive ions. The Franck-Condon transition model was proposed independently by Redhead[5] and by Menzel and Gomer.[14] Another mechanism was suggested recently by Knotek and Feibelman.[15] It involves the excitation of a core hole with subsequent deexcitation by either an interatomic or intra-atomic Auger decay. If the first mechanism holds also for the negative ion, the final state of the transition is the repulsive state between a negative ion and the substrate. The core-hole model would require a highly negatively polarized adsorbed oxygen atom to form an O^- after the Auger decay. This is not very probable for the loosely bound α state. In the absence of other detailed knowledge regarding the formation of negative ions, we shall use this

Franck-Condon mechanism as a guide.

According to the Franck-Condon principle, the IED is a reflection of the probability density distribution (PDD) of the vibrational ground state of the adsorbate-substrate oscillation, by the repulsive final-state potential curve. Ions desorbed at a smaller distance x_0 from the surface has a higher energy. However, owing to the interaction of the ion with the substrate, the IED is modified by a velocity-dependent neutralization factor. The probability of desorption of an ion starting from x_0 and moving to infinity without being neutralized[14] is

$$p_I(x_0) = \exp\left(-\int_{x_0}^{\infty} \frac{R(x)}{v}\,dx\right), \tag{1}$$

where $R(x)$ is the rate of neutralization of the ion at x and v is the velocity of the ion along the final-state potential curve. If this potential energy curve can be represented by

$$V = Be^{-bx}, \tag{2}$$

where B and b are constants, and if $R(x)$ can be expressed in the form

$$R(x) = Ae^{-ax}, \tag{3}$$

then

$$p_I(x_0) = \exp\left[-\frac{A}{b}\left(\frac{m}{2B}\right)^{1/2} \exp\left(-(a-\frac{b}{2})x_0\right) F(p,\infty)\right]. \tag{4}$$

Here $p = a/b$ and $F(p,\infty)$ is the incomplete Euler β function. The $m^{1/2}$ factor suggests an isotope effect of the desorption cross section. Madey *et al.*[16] observed that in the case of O^+, the $^{16}O^+$ desorption cross section for an oxygen covered W surface was about 1.5 times that of $^{18}O^+$. We also observed similar isotope effect for O^- and O^+ in our experiment. The $^{16}O^-$ saturation yield was also about 1.5 times that of $^{18}O^-$. It is possible that the O^- ions also had a velocity-dependent neutralization mechanism similar to that for positive ions. The dependence on x_0 is reflected by the dependence of p_1 on the energy of the desorbed ions. The IED is hence modified by this factor. An interesting implication is that the isotope effect would also be energy dependent. Madey *et al*,[16] reported that for oxygen chemisorbed on W, to within the precision of their measurement, the IED's of $^{16}O^+$ and $^{18}O^+$ were identical. This implies that $a \cong \frac{1}{2}b$.

We made a more detailed investigation of the energy dependence of the isotope effect. We observed a subtle difference in the shape of the IED's of the isotopes. Figure 5 shows the IED's of $^{18}O^+$ and $^{16}O^+$ together with the $^{18}O^+$ to $^{16}O^+$ ratio at various escape energies. The experiment was

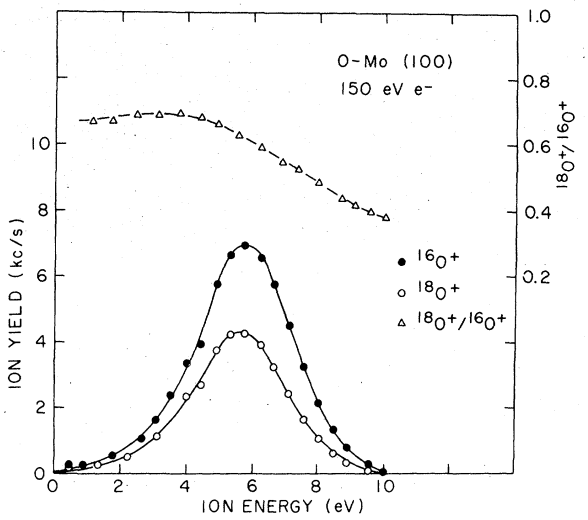

FIG. 5. $^{18}O^+$ and $^{16}O^+$ ion energy distributions. The $^{18}O^+$ to $^{16}O^+$ ratio at various ion energies shows the energy dependence of the isotope effect.

performed by coadsorbing a 1:1 $^{18}O_2$ and $^{16}O_2$ gas mixture on the Mo surface at room temperature. The exposure was about 6 L. The mass transmission of the mass spectrometer was programmed to alternate between $^{18}O^+$ and $^{16}O^+$ so that the IED's for both ions were monitored simultaneously without complications from work function corrections. A larger isotope effect was observed at the high-energy end. Figure 6 shows a similar observation with the $^{18}O^-$ and $^{16}O^-$ ions. Owing to the much smaller yields, the data were not as good as those of positive ions. The qualitative behavior as a function of ion energy, however, was not altered. This is another indication that the de-

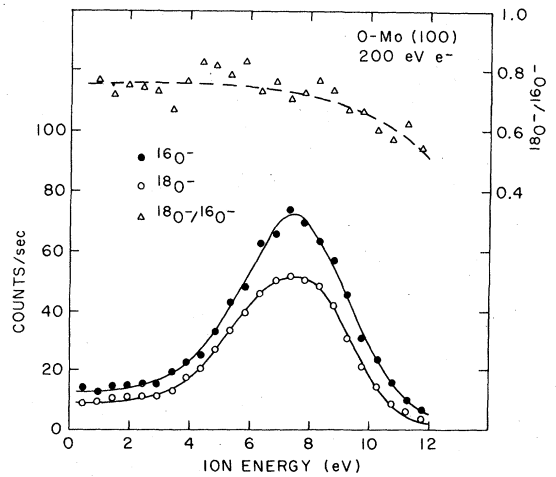

FIG. 6. $^{18}O^-$ and $^{16}O^-$ ion energy distributions. The $^{18}O^-$ to $^{16}O^-$ ratio also shows an energy dependence similar to that for O^+.

sorption mechanism of negative ions is very similar to that for positive ions.

There is one more isotope effect that we have to consider. The mass of the oxygen atom enters into the zero-point vibration frequency of the ground state. The ground state of the adsorbate-substrate harmonic oscillation amplitude is inversely proportional to the fourth root of the mass. Hence in between ^{18}O and ^{16}O, there is about a 3% difference in the spatial extend of the PDD, with the ^{18}O PDD being the more localized distribution. However, we should expect that the isotope effect would modify the IED's symmetrically about the distribution peak, which was not observed in the experiment. So unless the ground-state vibration is very anharmonic, the observed energy dependence of the isotope effect can be a consequence of the neutralization process discussed above.

When $a \neq \frac{1}{2}b$, the isotope effect is a function of energy through the dependence on x_0. Limited by the energy resolution of the energy analysis, we shall only make a rough comparison with the theory. Let us choose x_0 and $x_0 + d$ to be the spatial limits of the ground-state PDD. Ions excited at x_0 and $x_0 + d$ would be the ions at the two ends of the IED. From Eq. (4),

$$\frac{\ln\left(\frac{p_I(x_0) \text{ for } ^{18}O}{p_I(x_0) \text{ for } ^{16}O}\right)}{\ln\left(\frac{p_I(x_0+d) \text{ for } ^{18}O}{p_I(x_0+d) \text{ for } ^{16}O}\right)} = \exp\left[\left(\frac{a-b}{2}\right)d\right]. \quad (5)$$

Following Ref. (17), $d \simeq 0.2$ Å. Taking the $^{18}O^+$ to $^{16}O^+$ ratios at about zero and 10 eV, we estimated that

$$[\tfrac{1}{2}(a-b)]_{O^+} \cong 5.2 \text{ Å}^{-1}.$$

For O^-, by taking the $^{18}O^-/^{16}O^-$ ratios at about zero and 12 eV, we estimated that

$$[\tfrac{1}{2}(a-b)]_{O^-} \cong 3.6 \text{ Å}^{-1}.$$

In spite of the different excitation potential curves and neutralization mechanisms that the O^- and O^+ may have, $a > \frac{1}{2}b$ for both ion species. If we assume[5] that $b \simeq 4$ Å^{-1} in both cases,

$$a_{O^+} \cong 7 \text{ Å}^{-1}, \quad (6)$$

while

$$a_{O^-} \cong 6 \text{ Å}^{-1}. \quad (6')$$

These values of a fall in the right range of values as determined in many other experiments.[17]

Both the oxygen-coverage dependences of the ion yields and the isotope effect suggested that O^- and O^+ were desorbed by very similar processes. It is very probable that Franck-Condon transitions are responsible for O^+ and also O^- emission. As the chemisorption bond between the oxygen atom and the Mo substrate changes with coverage and temperature, the excitation cross sections to the repulsive potentials would be altered. Our observation of the variation in the O^- to O^+ ratio with temperature and coverage demonstrated that such cross-section changes were appreciable.

ACKNOWLEDGMENTS

The author would like to thank Dr. M. Strongin, Dr. R. Smith, Dr. R. Watson of BNL, and Dr. T. Madey of The Natl. Bur. Stand. for useful discussions, O. Kammerer and J. Hurst for preparation of the sample, and G. Hrabak for valuable technical assistance. The research was supported by the U. S. Department of Energy.

*Present address: IBM Thomas J. Watson Research Center, P. O. Box 218, Yorktown Heights, N. Y. 10598.

[1]T. E. Madey and J. T. Yates, Jr., J. Vac. Sci. Technol. 8, 525 (1971); D. Menzel, Surf. Sci. 47, 370 (1975).
[2]G. E. Moore, J. Appl. Phys. 30, 1086 (1959).
[3]A. Kh. Ayukhanov and E. Turmashev, Sov. Phys. Tech. Phys. 22, 1289 (1977).
[4]J. L. Hock and D. Lichtman, Surf. Sci. 77, L184 (1978).
[5]P. A. Redhead, Can. J. Phys. 42, 886 (1964).
[6]D. Lichtman and T. R. Kirst, Phys. Lett. 20, 7 (1966).
[7]P. H. Dawson, Phys. Rev. B 15, 5522 (1977).
[8]H. K. Kan and S. Feuerstein, J. Chem. Phys. 50, 3618 (1969).
[9]R. Riwan, C. Guillot, and J. Paign. Surf. Sci. 47, 183 (1975).
[10]T. E. Felter and P. J. Estrup. Appl. Surf. Sci. 1, 120 (1977).
[11]A modified version of the Bessel Box manufactured by Extranuclear Laboratories, Inc.
[12]T. Madey, Surf. Sci. 33, 355 (1972).
[13]M. L. Yu. Surf. Sci. 64, 334 (1977).
[14]D. Menzel and R. Gomer, J. Chem. Phys. 41, 2339; 41, 3311 (1964).
[15]M. L. Knotek and P. J. Feibelman, Phys. Rev. Lett. 40, 964 (1978); Phys. Rev. (to be published).
[16]T. E. Madey, J. T. Yates, D. A. King, and C. J. Uhlaner, J. Chem. Phys. 52, 5215 (1970).
[17]M. Nishijima and F. M. Propst, Phys. Rev. B 2, 2368 (1970).